J Mater Sci (2007) 42:4591–4602
DOI 10.1007/s10853-006-0575-9

Physical properties of low-*k* films based on the co-condensation of methyltrimethoxysilane with a bridged silsesquioxane

B. R. Kim · J. W. Kang · K. Y. Lee ·
J. M. Son · M. J. Ko

Received: 10 July 2005 / Accepted: 14 June 2006 / Published online: 16 February 2007

Abstract Though spin-on organosilicates are considered as the promising candidates of low dielectric constant materials, it is necessary for a successful integration to improve mechanical strength such as modulus and fracture toughness. In this study, five sets of MTMS–BTMSE copolymers were synthesized and characterized while the monomer content of BTMSE (bis(trimethoxysilyl)ethane) was varied from 9.1 to 47.3 mol% vs. MTMS (methyltrimethoxysilane). In parallel with the measurement of dielectric constant, four different tests were carried out to evaluate mechanical properties of the MTMS–BTMSE copolymers. Modulus was measured by the nanoindentation technique and the modified edge lift-off test (MELT) was employed to extract adhesive fracture toughness quantitatively. In addition, residual stress was calculated by sensing the change in radius of curvature of the substrate. The chemical structure of the copolymers was also analyzed with FTIR and NMR. Network formation was enhanced as the amount of BTMSE increased, which led to improvement of modulus and the increase in refractive index and dielectric constant. However, an increasing rate of fracture toughness by the MELT was not proportional to the increase in the amount of BTMSE, which implied that it was necessary to optimize the composition of the copolymers since adhesion strength was conjectured the most critical factor for a successful integration.

Introduction

As a feature size diminishes in the semiconductor chip, lowering interline capacitance and line resistance is required to reduce RC delay, power consumption and cross-talk. To address these problems, new materials with lower resistivity and dielectric constant should be developed as metal lines and interlayer dielectrics (ILD). While the only practical option replacing aluminum metal line is copper, the pursuit to substitute silicon dioxide is still in progress since the properties for low dielectric constant (low-*k*) ILD are so diverse and stringent. According to ITRS roadmap, dielectric constant suitable for 152 nm pitch is 2.4 in the year 2007 and the value required for 54 nm pitch should be smaller than 2.0 in the year 2016 [1].

Though dielectric constant is a primary factor to rank the performance of the low-*k* ILD, thermal and mechanical stabilities are also necessary for a successful integration into multilayer structures. However, lowering dielectric constant generally causes the detrimental effects on thermo-mechanical properties such as modulus, hardness, cohesion/adhesion strength, and thermal expansion coefficient. The deterioration of mechanical properties leads to film damage and/or delamination during the semiconductor fabrication processes such as chemical–mechanical planarization (CMP) or repeated thermal cure cycles. Therefore, it is necessary to minimize the degradation of mechanical properties along with an attempt of lowering dielectric constant.

According to the chemical structure, spin-on low-*k* materials are classified into two groups: organic polymers and organosilicates. Organic polymers generally

---

B. R. Kim (✉) · J. W. Kang · K. Y. Lee ·
J. M. Son · M. J. Ko
LG Chem. Ltd., Research Park, 104-1 Moonji-dong,
Yuseong-gu, Daejeon 305-380, Korea
e-mail: brkim@lgchem.com

have a low dielectric constant but show somewhat high thermal expansion coefficient as well as low mechanical strength. The addition of fluorine into organic polymers contributes to lower the dielectric constant further, but gives a harmful effect on thermal stability and interface adhesion. To improve adhesion strength, adhesion promotor is normally used at the interface of polymers and metal layers. Organic–inorganic hybrid materials, or organosilicates has the higher mechanical strength and dielectric constant than the organic counterparts since their chemical structures consisted of O–Si–O backbones are similar to inorganic silica. They normally have a good gap-fill capability, high thermal stability, and a good resistance to chemical attacks. The dielectric extendibility to materials with lower dielectric constant is generally achieved by introducing porosity into organosilicates [2–4]. However, the reduction in film density caused by the incorporation of voids is accompanied by the deterioration of mechanical strength, which provides a number of integration challenges. In order to improve mechanical strength of porous organosilicates, the effort to search for base materials with lower polarizability is necessary to minimize the pore contents.

Among several organosilicates, MSSQ (methyl-silsesquioxane) exhibits numerous desirable properties that are needed for a viable low-*k* material. The bulky organic groups contribute to reduce polarizability and to establish microporosity so that dielectric constant is in the range of 2.6–2.8 [2, 3]. Though hydrogen-silsesquioxane (HSSQ) has been considered as a promising candidate material [5], it is known that HSSQ is less stable than MSSQ under oxidative conditions. While Si–C bonds are more robust and CH_3 groups in MSSQ are more hydrophobic, the weak Si–H bonds in HSSQ are susceptible to cracking and moisture uptake, which increases dielectric constant. In addition, MSSQ films tend to have lower stress and higher resistance to cracking when compared to HSSQ [6]. However, the low modulus of MSSQ can be a major obstacle for the implementation in the next generation of devices and still remains to be improved.

In this study, MTMS (methyltrimethoxysilane) monomers were copolymerized with BTMSE (bis(trimethoxysilyl)ethane) monomers for the improvement of physical properties, especially in mechanical properties. Compared with MSSQ, it is likely that MTMS–BTMSE copolymers have better mechanical properties since the addition of BTMSE with greater functionality than MTMS enhance network formation. In spite of this advantage, the introduction of carbon bridges has a possibility of increasing unreacted functional endgroups and causing a harmful effect on dielectric constant. Kim et al. lately reported that the modulus of the MTMS–BTMSE (9:1 mol%) copolymer film was twice greater than that of MSSQ at the increase in dielectric constant from 2.70 to 2.86 [7].

Though the increase in the BTMSE content improved mechanical properties of the copolymer film, the trend cannot last eternally, which means that it is necessary to find the adequate amount of BTMSE that can optimize physical properties. Therefore, current study extended the experiments and is attempted to find proper amount of BTMSE. In order to investigate the effect of BTMSE on physical properties, five sets of MTMS–BTMSE copolymers were synthesized while the monomer content of BTMSE was varied from 9.1 to 47.3 mol% vs. MTMS. The copolymers were synthesized by the sol–gel reaction and dispersed on blanket wafers by spin coating. This systematic investigation of MTMS–BTMSE copolymers is expected to assist in finding the adequate amount of BTMSE that can optimize mechanical properties along with dielectric constant. In addition, the selected copolymer can be used as a base matrix material when reducing dielectric constant through incorporation of porosity.

Experimental

Material synthesis and film processing

A flame dried flask was charged with vinyltrimethoxysilane (296.5 g, 2.0 mol, Aldrich), and platinum(0)-2,4,6,8-tetramethyl-2,4,6,8-tetravinylcyclotetrasiloxane complex (1.0×10^{-6} m^3, 0.104 M solution in methylvinylcyclosiloxane, Aldrich) under dry nitrogen. While being stirred at room temperature, trimethoxysilane (268.8 g, 2.2 mol, Tokyo Kasei Kogyo Co., Ltd.) was slowly added to the reaction mixture by a cannula, and then allowed to warm up to 60 °C. The reaction mixture darkened within a few minutes at 40 °C was stirred over 8 h at 60 °C. After 8 h, the dark liquid was vacuum distilled (26.7 Pa, 100 (C), yielding a clear, colorless BTMSE solution (524.6 g, 1.94 mol, 97%): ^1H NMR (300 MHz, solid MAS probe at static condition): $\delta = 3.57$ (s, 18H, OCH_3), 0.59 (s, 4H, $SiCH_2CH_2Si$). ^{13}C NMR (75 MHz, solid MAS probe at static condition): $\delta = 49.68$ (OCH_3), 0.11 ($SiCH_2CH_2$-Si). ^{29}Si NMR (99 MHz, solid MAS probe at static condition): $\delta = -41.96$.

The BTMSE solution with 9.1–47.3 mol% was mixed with MTMS to form MTMS–BTMSE copolymer solutions shown in Fig. 1. Different from MSSQ consisted of with O–Si–O backbone only, the MTMS–BTMSE copolymer was partially connected to O–Si–

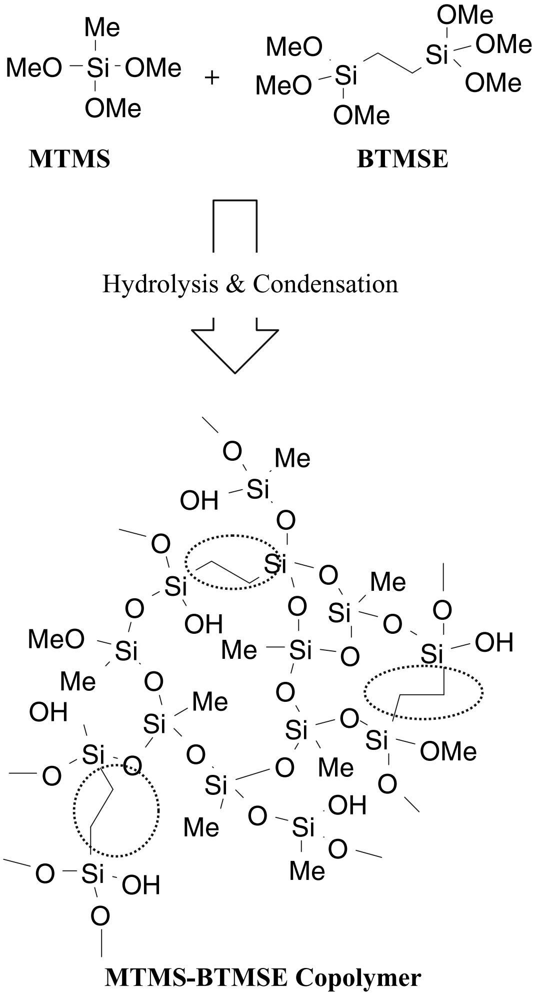

Fig. 1 Schematics of MTMS–BTMSE copolymer

CH_2-bond as outlined in Fig. 1 by a dotted border. Each of the silicate pre-polymer solutions was prepared under the acidic conditions. First, MTMS and BTMSE pre-polymers were mixed with deionized water and solvent with stirring. About 3.0 equivalent of deionized water per each alkoxy group was added and the concentration of reaction mixture was adjusted to 2.07 M by water and propyleneglycol methylether. Second, deionized water including 1×10^{-2} equivalent of HNO_3 was added to this solution at room temperature and stirred for 30 min or longer. This mixture was stirred at 60 °C over 15 h and then cooled to room temperature. Finally, to this mixture was added additional propyleneglycol methylether, generally of the same amount of initial value. Low boiling point solution containing EtOH and water was removed from the reaction mixture by vacuum evaporation at 45 °C leading to the final coating solution containing a condensate with a weight average molecular weight of 1,000–5,000. The molecular weights were measured by gel permeation chromatography (VISCOTEK) based on PS standards.

The coating solution was applied to a 127 mm (5 in.) silicon wafer with a spin coater at an acceleration rate of 1,000 rpm/s and a spinning rate of 2,000 rpm/s for 30 s. After deposition, the film on wafer was dried for 2 min on a hot plate maintained at a temperature of 100 °C to thereby remove the organic solvent. Subsequent annealing was usually performed for 60 min at 430 °C under N_2 environment, leading to form a colorless transparent film. The film thickness ranged from less than 500 nm up to 2,000 nm, depending on the spin speed and the solid content of coating solution.

Property characterization

Valuable information about the chemical structure of the film can be obtained by means of solid state ^{29}Si nuclear magnetic resonance (NMR, Bruker DSX300) spectroscopy. In order to avoid the line broadening effects generated through strong dipolar–dipolar and chemical shift anisotropy interactions, the magic angle spinning (MAS) technique was employed. The ^{29}Si MAS NMR spectra provided information on the distribution of silicon species present and the change of silicon species during thermal cure. Fourier-transform infrared (FT-IR, Bio-Rad FTS3000) spectroscopy was also performed in the mid-infrared region (4,000–400 cm^{-1}) which corresponded to the vibrational frequency of molecules. The spectra were mainly used to identify the chemical species present and compare the relative magnitude of absorption peaks of each copolymer.

Refractive index and film thickness were extracted by ellipsometry (Jobin Yvon UVISEL^{TM}) that was very sensitive and non-destructive method suited for the investigation of transparent films. The calculation of refractive index and film thickness was based on curve-fitting with the phase and amplitude ellipsometric angle Ψ and Δ measured at 70° fixed angle of incidence and 632.8 nm wavelength. Dielectric constants of low-*k* films were determined with metal–insulator–semiconductor (MIS) structures by impedence analyzer HP 4194A. After aluminum electrode was deposited on low-*k* films with the electron beam evaporator, electrical capacitance was measured while DC voltage was swept from –40 to 40 V. The dielectric constant was calculated from the known relationship between thickness and capacitance.

Elastic modulus and hardness were obtained using the continuous stiffness measurement (CSM) technique on a MTS nanoindenter XP equipped with the DCM head [8]. In this technique, an extremely small sinusoidal oscillation was superimposed on the load ramp and the dynamic response of the contact was determined, which allowed the hardness and modulus of the material to be continuously obtained throughout the indentation process. The test was carried out at 75 Hz fixed frequency and with Berkovich(three-side pyramid shape) indenter. Six indentations were performed on each sample up to 200 nm depth and averaged.

Residual stress was evaluated by Tencor FLX-2320 system that employed a laser scanning technique to sense deformation caused by thin films on a wafer [9]. Since every wafer had some initial curvatures and surface irregularities, measures were taken before and after films were deposited. This change in curvatures of the wafer could be converted into residual stress of thin films employing the following Stoney's equation

$$\sigma = \frac{E_s t_s^2}{6(1 - \nu_s) t_f} \left(\frac{1}{R} - \frac{1}{R_0} \right), \tag{1}$$

where σ is the film stress, E_s is the elastic modulus of the substrate, ν_s is the Poisson's ratio of the substrate, R_0 is the radius of curvature of the bare wafer, R is the substrate radius of curvature of the film on the wafer, t_s is the substrate thickness, and t_f is the film thickness.

The modified edge lift-off test (MELT) method was adopted to determine and compare fracture strength of low-k materials [10]. Figure 2 illustrates the general procedure of the MELT that was utilized to measure fracture toughness. Epoxy backing layer applied onto low-k films increased energy stored in the system, and it made the films debonded from the substrates without going to an extremely low temperature. Since the backing layer was much thicker than low-k films, the total energy for delamination was approximately equal to the energy of the backing layer. Therefore, fracture toughness can be expressed as the following equation

$$K_{IC} = \sigma_0 (h_0/2)^{0.5}, \tag{2}$$

where σ_0 is the residual stress of the epoxy, and h_0 is the thickness of epoxy backing layer.

A couple of samples with the size of 50 × 50 mm^2 cleaved from the original wafer were coated with epoxy and cured at 180 °C in the air. The larger samples were diced onto a square shape of an area 13 × 13 mm^2 for the test and 18 small samples for each copolymer were collected. Since up to 30 samples per cycle were allowed to be tested in the cryostat chamber, six samples from each copolymer were selected and placed into the chamber. After the same tests were repeated three times, all data were averaged to calculate fracture toughness. After testing, the sample surface was examined to verify the onset of delamination and crack path by direct visual inspection or through the X-ray photoelectron spectroscopy (XPS).

Results

Chemical structure analysis

Figure 3 represents solid state ^{29}Si MAS NMR spectra of as-synthesized and the cross-linked MTMS–BTMSE copolymers after 430 °C cure. For the analysis of spectra, the fitting was performed with Gaussian lineshapes in Bruker Win-NMR data processing program. The peak numbers were specified and the peak positions were roughly designated initially for the deconvolution with Gaussian lineshapes. Chemical structures of each copolymer could be induced from the relation between the average Si–O–Si intertetrahedral angles and the typical chemical shift δ obtained by ^{29}Si MAS NMR. Based on the chemical shift δ of trifunctional groups, T^n [T^1 (–47 ppm), T^2 (–57 ppm), T^3 (–64 ppm)], the percentage of functional endgroups in each copolymer was calculated, which was summarized in Table 1. As BTMSE contents increased, the percentage of functional endgroups in as-synthesized copolymers increased gradually, and finally reached one functional endgroup (–OH or –OMe) per almost one Si atom for MTMS:BTMSE = 100:90 copolymer. It was clear that the multifunctional monomer, BTMSE, interrupted the sol–gel polymerization with its hindered structure under the given conditions, so that more unreacted functional endgroups remained in the as-synthesized copolymers with the increase in the proportions of BTMSE. These residual functional endgroups induced the intermolecular condensation during thermal cure process and affected the final film density and mechanical properties. As expected, 430 °C curing led to an increase in the T^3 unit and a decrease in the T^1 and T^2 units. Surprisingly, the degree of condensation for the T unit was similar between MTMS:BTMSE = 100:30, 100:50, and 100:70 copolymers. They had approximately one defect functional endgroups per five silicon atoms while 100:10 had one per ten silicon atoms. In general, the increase in BTMSE amount elevated the defect functional endgroups as well as promoted condensation reaction that resulted in the increase in a cross-linking density.

FT-IR spectra of MTMS–BTMSE copolymers before and after 430 °C thermal cure process are presented in

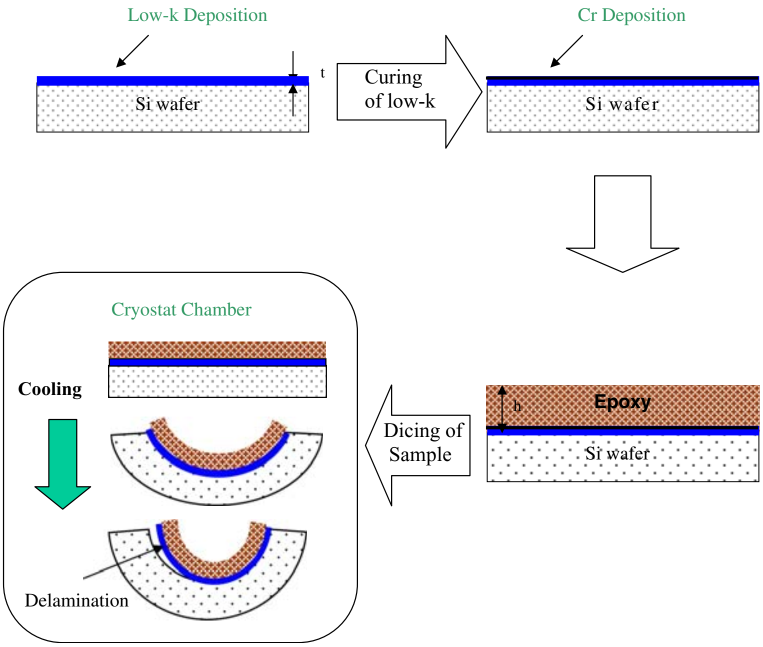

Fig. 2 Schematics of MELT test structure to calculate fracture toughness

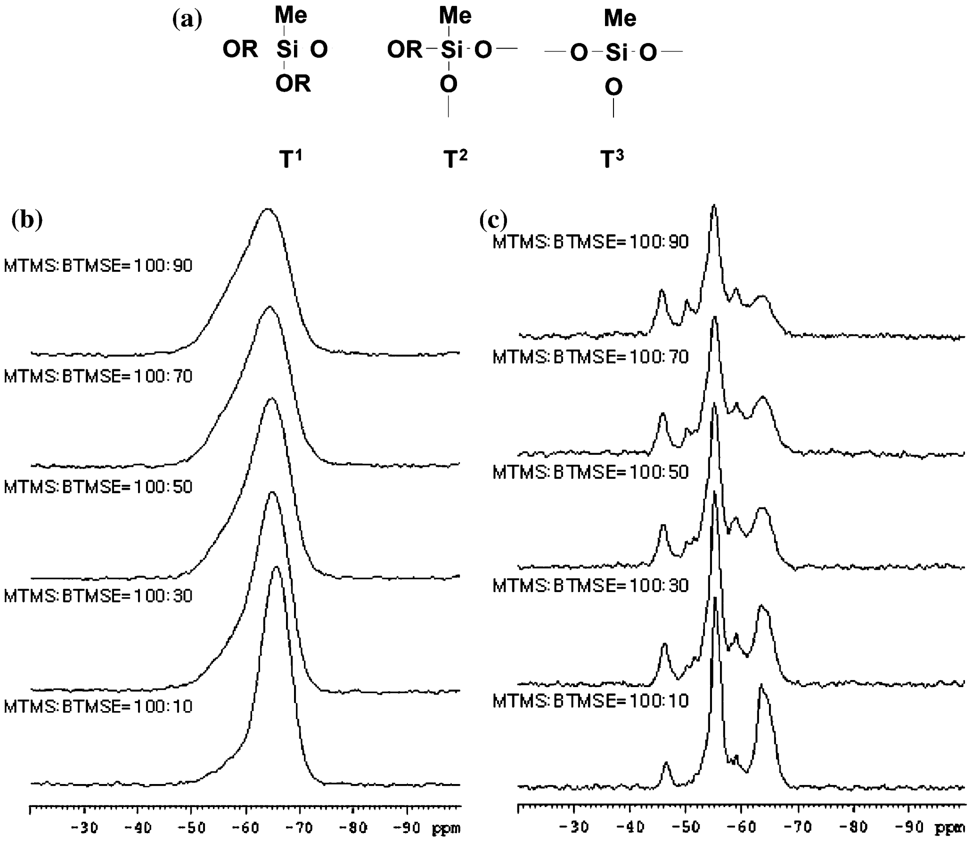

Fig. 3 (**a**) The structures of trifunctional group investigated in MTMS–BTMSE copolymers, (**b**) the solid state ^{29}Si MAS NMR spectra of as-synthesized copolymers, (**c**) the solid state ^{29}Si MAS NMR spectra of the cross-linked copolymers after 430°C cure

Fig. 4. For clarity, the relative intensities (transmittance) were offset vertically. Molecular formula of the copolymers were similar to those of SiO_2 except the fact that some oxygen atoms on side and main chains in SiO_2 were replaced by –OH, –OCH_3, –CH_3, or –CH_2CH_2– bridges. The characteristic peaks of the copolymers were CH_2–CH_2 rocking vibration peak, siloxane structure peak (O–Si–O) and three methyl group (Si–CH_3) peaks. While the intensity of CH_2–CH_2 peak located near 730 cm^{-1} was directly related to the amounts of

Table 1 The percentage of functional endgroups of as-synthesized and the cross-linked MTMS–BTMSE copolymers after 430 °C cure

Composition	Status	T^1	T^2	T^3	f.e
MTMS:BTMSE = 100:10	As-synthesized	5.0%	56.7%	38.3%	66.7%
	After 430 °C cure	–	11.5%	88.5%	11.5%
MTMS:BTMSE = 100:30	As-synthesized	8.7%	63.6%	27.7%	81.0%
	After 430 °C cure	–	19.6%	80.4%	19.6%
MTMS:BTMSE = 100:50	As-synthesized	9.3%	65.0%	25.7%	83.6%
	After 430 °C cure	–	20.8%	79.3%	20.8%
MTMS:BTMSE = 100:70	As-synthesized	9.8%	64.9%	25.3%	84.5%
	After 430 °C cure	–	21.2%	78.8%	21.2%
MTMS:BTMSE = 100:90	As-synthesized	12.3%	67.3%	20.4%	91.9%
	After 430 °C cure	–	23.1%	76.9%	23.1%

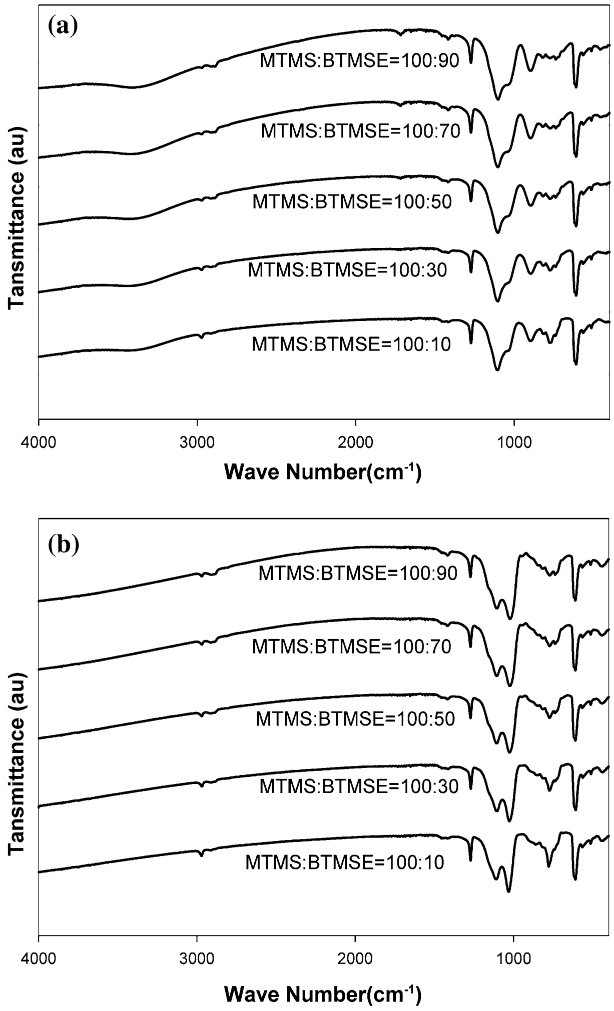

Fig. 4 FT-IR spectra for MTMS–BTMSE copolymers with different compositions (**a**) before thermal curing, (**b**) after 430 °C thermal cure process

BTMSE monomer, the transmittance of methyl groups located at 2,970 cm^{-1} (CH_3 stretching), 1,273 cm^{-1} (CH_3 deformation) and 779 cm^{-1} (Si–C stretching) was proportional to the contents of MTMS. The trend stayed unchanged after 430 °C thermal cure process, which suggested that Si–CH_3 groups and bridged carbon chain were stable over 430 °C under a nitrogen atmosphere.

In order to make a comparative study of chemical structures before and after 430 °C thermal cure, the FT-IR spectra for MTMS:BTMSE = 100:10 and MTMS:BTMSE = 100:90 are redrawn in Fig. 5 in a specified range (800–1,400 cm^{-1}). Siloxane structures were characterized by peaks at 1,100–1,130 cm^{-1} and 1,020–1,050 cm^{-1}, depending on their structures and chain length. After thermal cure process, a dramatic peak shift was observed from 1,105 to 1,025 cm^{-1}. This result illustrated that siloxanes went through the structure rearrangement of random network and the excessive increase of chain length by high molecular weight gel formation. The degrees of peak shift were consistent with the order of BTMSE content. Silanol group, Si–OH found at 897 cm^{-1}, almost disappeared after thermal cure process, which indicated that the condensation cross-linking reaction of the MTMS–BTMSE copolymers effectively proceeded in the given curing conditions. These results corresponded to the

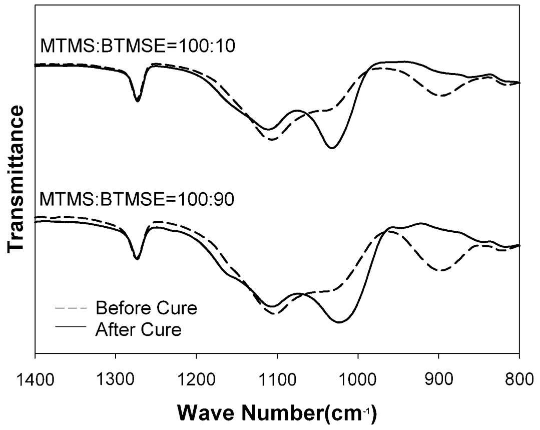

Fig. 5 FT-IR spectra for MTMS:BTMSE = 100:10 and MTMS:BTMSE = 100:90 in a specified range

previous NMR study, and could assist to understand the trends in electrical and mechanical properties.

Dielectric constant

It is known that both electronic and nuclear polarizations affect the dielectric constant at typical device operating frequency. Since electron, the lowest mass of species, can align fast enough to keep up with the applied electric field, the electronic polarization response dominates at high frequency and its magnitude is associated with the refractive index according to $k_e = n^2$. On the other hand, the nuclear response becomes more important at lower frequencies since the polarization of dipoles requires more time than electronic polarization. Therefore, the magnitude of electronic component is affected by bond strength and that of the nuclear component is dominated by the polar substituents such as hydroxyl and carboxyl groups. The separate calculations of both components may lead to understanding how the molecular structure influences dielectric properties of low-*k* films.

The dielectric constant of SILK (Trademark of The Dow Chemical Company) was determined mainly by the electronic component since the aromatic hydrocarbon resin did not contain any polar substituents [11]. In contrast, the magnitude of the nuclear component in silicon dioxide was relatively high due to the strong atomic polarization, and it was nearly the same as that of the electronic component. This trend could be also applied to other organic polymers and inorganic materials. For organic–inorganic hybrids, the percentage of the nuclear component in the dielectric constant was located between those of SILK and silicon dioxide. The percentage of the nuclear component of MSSQ with one methyl group in each silicon atom corresponded to 25% of the dielectric constant.

Table 2 lists the electronic and nuclear components of each MTMS–BTMSE copolymer, which were calculated from the measured refractive indices and dielectric constants. For comparison, the values of MSSQ are also presented. As the proportions of BTMSE to MTMS increased, both the components steadily increased the properties slower than linearly. As shown in the previous NMR results, the increase in the electronic component in proportion to BTMSE content could be attributed to the increase in the percentage of functional endgroups. Not only did the increase in the percentage of functional endgroups promote further condensation reaction, but also the flexibility of carbon backbone enhanced the possibility of cross-linking by bringing separate pre-polymers to easily access. In other words, the improvement in bond density could be accomplished both by forming O–Si–O bond through the condensation reaction of functional endgroups and by binding up two separately condensed structures which resulted in enhancing the connectivity within the films. While the electronic component of the copolymers was closely related to the bond density, unreacted functional endgroups remained after cure contributed to elevate the nuclear component. The previous NMR result proved that the percentage of the defect functional groups was also proportional to the amount of BTMSE. Interestingly, there were few, if any, differences in the electronic to nuclear component ratio of the copolymers regardless of chemical compositions. In other words, the addition of supplementary BTMSE influenced the enhancement of bond density and the increase in defect functional groups at the same rate. Considered that there was a trade-off in decreasing the electronic component and desirable mechanical properties, the minimization of the defect functional groups would be a key factor to obtain desirable dielectric constant without much sacrificing mechanical properties.

Mechanical properties

Mechanical reliability of low-*k* films cannot be characterized by a single quantity since mechanical and thermal histories of each fabrication process were different, which caused diverse failure behaviors. Table 3 summarizes four representative mechanical properties measured to characterize the copolymer low-*k* films. Mechanical properties of MSSQ are also listed for comparison. In spite of some interrelationships between the mechanical properties, they had their inherent physical meanings and so should be measured

Table 2 Dielectric constants and refractive indices of low-*k* candidates

Composition	n	k	$k_e = n^2$	$k_n = k - n^2$
MSSQ (MTMS only)	1.385	2.73 ± 0.03	1.918(71.3%)	0.812(29.7%)
MTMS:BTMSE = 100:10	1.415	2.76 ± 0.01	2.002(72.5%)	0.758(27.5%)
MTMS:BTMSE = 100:30	1.431	2.83 ± 0.02	2.048(72.4%)	0.782(27.6%)
MTMS:BTMSE = 100:50	1.441	2.88 ± 0.02	2.076(72.1%)	0.804(27.9%)
MTMS:BTMSE = 100:70	1.446	2.90 ± 0.02	2.091(72.1%)	0.809(27.9%)
MTMS:BTMSE = 100:90	1.450	2.92 ± 0.02	2.103(72.0%)	0.828(28.0%)

Table 3 Mechanical properties of MTMS–BTMSE copolymers

Composition	Reduced modulus (GPa)	Hardness (GPa)	Residual stress (MPa)	K_{IC} (MPa $m^{0.5}$)
MSSQ(MTMS only)	4.1 ± 0.1	0.60 ± 0.02	54.1 ± 0.6	<0.13
MTMS:BTMSE = 100:10	6.6 ± 0.1	0.91 ± 0.14	58.4 ± 1.2	0.166 ± 0.003
MTMS:BTMSE = 100:30	9.7 ± 0.1	1.37 ± 0.21	70.8 ± 1.4	0.191 ± 0.003
MTMS:BTMSE = 100:50	11.7 ± 0.2	1.66 ± 0.07	92.3 ± 1.3	0.202 ± 0.003
MTMS:BTMSE = 100:70	13.1 ± 0.2	1.77 ± 0.14	109.2 ± 1.5	0.210 ± 0.010
MTMS:BTMSE = 100:90	14.3 ± 0.2	1.90 ± 0.07	117.5 ± 1.4	0.208 ± 0.009

separately. While modulus was the quantity to characterize film itself, the others were influenced by the substrate and the film/substrate system. The detailed analyses of each mechanical property for MTMS–BTMSE copolymers would be addressed individually.

Though the most appropriate way to measure basic mechanical properties would be the tensile test of free-standing films, it was not normally chosen for characterizing low-*k* films since it was difficult to detach the films from the substrate without any damage or deformation. Surface acoustic wave spectroscopy (SAWS) [12] and the beam bending method [13] have been considered to measure the modulus of low-*k* films indirectly but the nanoindentation technique has been the popular method to measure the modulus since this method did not need any sample preparation and could be carried out quickly and inexpensively. Traditionally, the indentation method has been used for the measurement of hardness that indicated a resistance to permanent deformation. After load and penetration depth could be recorded at each load increment, this method became the versatile technique for measuring various mechanical properties of films such as modulus, fracture toughness, yield strength, etc. In this study, modulus and hardness were obtained using the continuous stiffness measurement (CSM) technique on a MTS nanoindenter XP equipped with the DCM head. While the modulus was considered as one of the basic properties to characterize an elastic behavior of materials, hardness was normally used to characterize the inelastic behavior of materials.

Figure 6a plots applied load vs. normalized indented depth curves for 200 nm peak indentation displacement in the MTMS:BTMSE = 100:10 and 100:90 copolymer films. The indentation traces of other copolymer films were located between the two. Indented depth of the films was so small that elastic contact was dominant and the mode of plastic deformation could hardly occur. In the situation, hardness did not provide any information about plastic properties and became proportional to modulus. Figure 6b shows the reduced modulus as a function of normalized indented depth, which was calculated by using the load–displacement curves. Regardless of compositions of the films, the profile took the shape of a checkmark. It is presumed that the high values observed at shallow depth were due to tip adhesion, indentation size effect, erroneous area function, or additional layer on low-*k* film such as oxide layer [14]. Meanwhile, the gradual escalation in modulus with the increase in indented depth was definitely attributed to the substrate effect, which explained that the indented depth was normally restricted to no more than 10% of film thickness. By averaging the values at a plateau region where the modulus was free from the low depth and substrate effects, the genuine modulus of the film could be obtained. However, it was difficult to characterize the intrinsic moduli of the current copolymer films since the modulus profiles did not have any plateau region and started to steadily rise from the very shallow indented depth. Therefore, the minimum values observed in the profiles were conventionally regarded as the genuine moduli of the copolymer films, which were summarized in the second column in Table 3.

As discussed earlier, the addition of BTMSE increased the percentage of functional end groups and then resulted in the higher degree of cross-linking. Considered that the excessive amount of BTMSE not only enhanced bond density but also increased unreacted functional groups, the increase in modulus was not always proportional to the amounts of BTMSE to MTMS. Rather than the amounts of BTMSE, the modulus was closely connected to the refractive index since both properties were influenced by the degree of cross-linking or bond density. The constant electronic to nuclear component ratio in BTMSE copolymers led to the linear relation between the dielectric constant and the refractive index. Due to these close correlations among the three mechanical, optical, and electrical properties, it was difficult to obtain low dielectric constant and desirable modulus simultaneously unless there were any auxiliary attempts to decrease the unreacted functional groups. Lately, the electron beam treatment or UV curing method was performed to

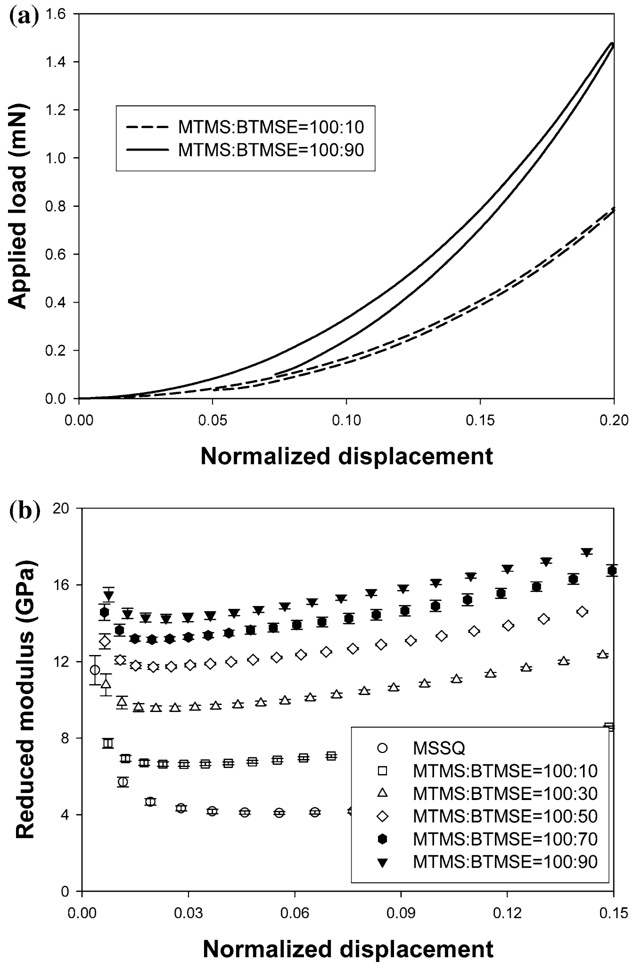

Fig. 6 Nanoindentation test result of MTMS–BTMSE copolymers with different composition. (**a**) Load vs. normalized indented depth curve for 200 nm peak indentation displacement in the MTMS:BTMSE = 100:10 and 100:90 copolymer films, (**b**) reduced moduli as a function of normalized indented depth

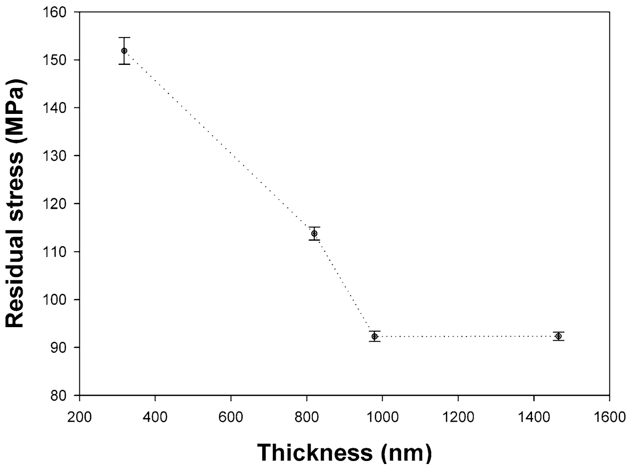

Fig. 7 Effect of film thickness on the residual stress in MTMS:BTMSE = 100:50 copolymer

improve cross-linking density by reacting the defect functional groups deliberately [15].

The residual stress of thin films, one of the properties of films that could impact the device reliability and lifetime was normally originated from a mismatch in the thermo-mechanical properties of interfaced layers such as modulus, Poisson's ratio, and thermal expansion coefficient. Before proceeding to comparison between MTMS–BTMSE copolymers, the effect of film thickness on the residual stress was investigated in advance. Figure 7 shows the variation in the residual stress for MTMS:BTMSE = 100:50 copolymers in thickness from 300 to 1,500 nm. The residual stress varied slightly on the films with thickness greater than 1 μm while the film of 300 nm thickness represented a very high stress. The residual stress for the films of thickness higher than 2 μm could not be measured due to an inferior coatability and stress-induced cracks on the surface. The similar stress-thickness behaviors (fast increase at small thickness, constant at moderate thickness, and stress induced cracking at higher thickness) were investigated for other MTMS–BTMSE copolymers.

It has not been clearly explained why the residual stress increased with decreasing thickness. Oh et al. urged that the high residual stress in the thinner film of MSSQ was attributed to a loosely packed morphological structure [16]. However, this conclusion was different from the general observation that the modulus at thinner films was inversely proportional to film thickness. On the contrary, the fact that temperature-residual stress profile of 200 nm thickness film deviated from the linearity hinted at the inhomogeneity of the film. Lee et al. reported that 19–30 nm thick denser surface layer on low-*k* film as well as oxide layer at the interface between the low-*k* film and wafer were observed in porous HSQ film [17]. Nay et al. also proposed the possibility of the existence in hard surface layer on low-*k* films [18]. When the thickness of surface layer was comparable to that of low-*k* films, Eq. 1 derived under the assumptions of homogeneity could generate an erroneous result.

In order to minimize the surface layer effect, the residual stress of each MTMS–BTMSE copolymer was estimated for films of thickness greater than 1.2 μm and listed in Table 3. The residual stress of MTMS:BTMSE = 100:10 was comparable to that of SILK dielectric resin (trademark of The Dow Chemical Company) in spite of the big disparity in their thermo-mechanical properties. Considered that there existed the substantial differences between the modulus of the two, it could be inferred that the thermal expansion coefficient of the copolymer might be two or three times smaller than SILK.

Table 3 also implies that the variation in BTMSE content had a minor effect on the thermal expansion coefficient. Since the variation of the thermal expansion coefficient on the increase in cross-linking density could not surpass the increase in the modulus, the residual stress seemed to steadily increase as the BTMSE content increased. From the information that the high residual stress exerted an additional driving force for delamination, it was recommended that the stress in low-*k* films be less than 100 MPa. Unless the improvement in the fracture strength caught up with the increase in residual stress, the copolymer films with higher percentage of BTMSE might face mechanical failures during fabrication process.

Though the MELT method has been widely used to measure adhesion strength at the interface, it could not be ensured that delamination always occurs at the interface. Since the onset and propagation of cracks were dependent on several factors such as toughness of low-*k* films, the adhesion strength, and mode mixty, samples should be inspected after testing to trace failure path and to examine the failure mechanism. While relatively thick residual thickness left on the Si substrate was an evidence of a cohesive failure, a mirror smooth Si surface indicated an adhesive failure. Except MTMS:BTMSE = 100:90 sample, most of the tested samples had mirror surfaces and their residual film thickness was expected to be less than 10 nm.

In order to verify this expectation, the thickness of every specimen was inspected after testing with XPS analysis that was the powerful method to quantify the residuals on the silicon. Figure 8 plots a profile of the chemical composition of MTMS:BTMSE = 100:50 sample as a function of etching depth, and the trend was nearly the same for the other samples. With 0.1 nm/s etch rate, XPS data were acquired between each etch period by scanning across the sample. Though carbon, oxygen, and silicon were detected on the surface, the carbon content rapidly decreased to 10% of initial content within 10 s etch and almost disappeared after 40 s etch. Considering that most of the samples had oxygen and carbon at the surface, the difference in chemical composition within the film thickness of 4 nm might be caused by the contamination from the atmosphere and handling, which implied that adhesive failure was the dominant failure mechanism for the copolymers.

The fourth column in Table 3 lists the fracture toughness measured by the MELT method. The addition of multifunctional monomer, BTMSE, lowered the numbers of hydrophobic carbon endgroups and then improved adhesion strength. Since delamination of MSSQ homopolymer occurred at room temperature during dicing, exact fracture toughness could not be measured but its value was smaller than 0.14 MPa $m^{0.5}$. The addition of 10% BTMSE to MTMS brought about a considerable improvement in fracture toughness whose value reached 0.166 MPa $m^{0.5}$, and the value increased steadily until the amount of BTMSE reached to 70% to MTMS. It was clear, however, that the effectiveness of BTMSE to fracture toughness decreased as its amount increased, which was almost the same tendency as that of modulus.

The increase in fracture toughness could not be continued for MTMS:BTMSE = 100:90 for which delamination did not occur at the interface. As the amount of BTMSE increased, it was very difficult to obtain accurate adhesion fracture toughness since cracks were not confined into the region of interest but

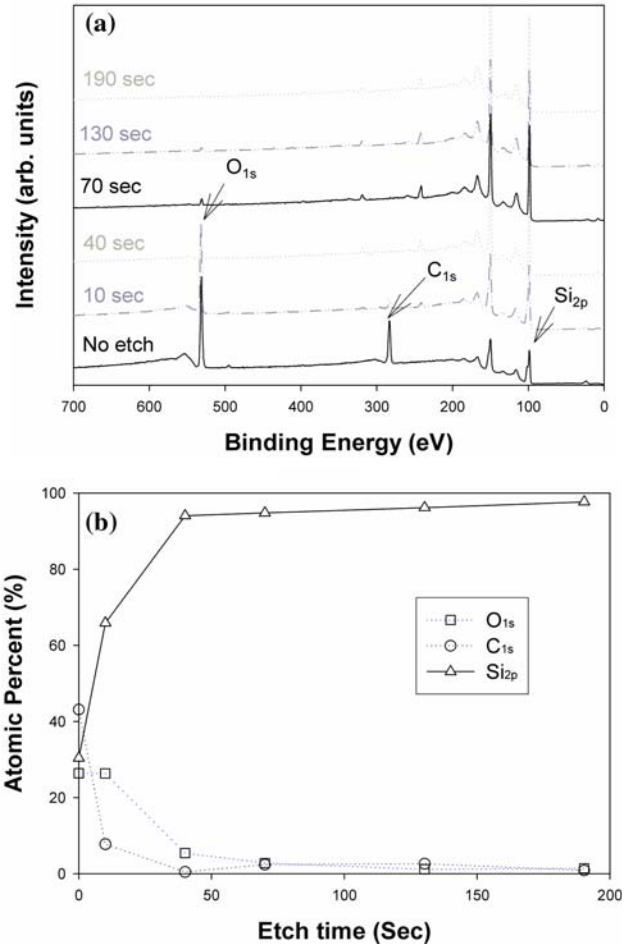

Fig. 8 XPS result for MTMS:BTMSE = 100:50 copolymer sample. (**a**) Relative numbers of each atoms vs. etch depth, (**b**) atomic percent of three atoms vs. etch depth

altered their directions frequently [19]. In this case, fracture toughness may represent or reflect cohesive strength of low-*k* materials. It implied that higher amounts of BTMSE did not always have an advantage of improving toughness.

Conclusions and summary

In this paper, MTMS–BTMSE copolymers were proposed as new low-*k* dielectric candidates and characterized by laying emphasis on mechanical properties. Focused on the effect of the carbon bridge, five sets of copolymers with a range of BTMSE monomer content were synthesized and explored.

- The addition of BTMSE with greater functionality than MTMS promoted the condensation reaction, which resulted in the increase of cross-linking density. The augmented flexible carbon backbones also played an important role to increase the cross-linking density within the films by connecting two separately condensed structures. FT-IR spectra represented that the degrees of siloxane peak shift from 1,105 to 1,025 cm^{-1} after cure were consistent with the order of BTMSE content.
- As the amounts of BTMSE increased, not only the electronic component related to cross-linking density but also the nuclear component of dielectric constant increased. This was mainly due to the increase in remaining defect functional endgroups after cure. Since there was a trade-off in decreasing the electronic component and obtaining desirable mechanical properties, the minimization of the defect functional groups would be a key factor to obtain a reasonable dielectric constant without much sacrifice in mechanical properties.
- For MTMS–BTMSE copolymer films, modulus measured by the nanoindentation technique was proportional to the percentage of functional endgroups rather than the amounts of BTMSE. The residual stress and the adhesion fracture toughness expressed the same trends. As the cross-linking density increased, the residual stress also steadily increased since the increase in the modulus overwhelmed the variation of the thermal expansion coefficient. Since the superior reactivity of methoxy and hydroxy groups to the silicon substrate enabled to form strong interfacial bonds, adhesion fracture toughness became proportional to the percentage of functional end groups.
- Except MTMS:BTMSE = 100:90 sample, the adhesive failure was the dominant failure mechanism for most of the tested samples. The addition of BTMSE improved the adhesion strength but the effectiveness of BTMSE decreased as its amount increased, which was almost the same tendency as that of modulus. For MTMS:BTMSE = 100:90 sample, fracture calculated toughness was not pure adhesive strength but might represent or reflect the cohesive strength of the sample since cracks were not confined into the region of interest.
- It has been known that the incorporating porosity into the base matrix material was indispensable to acquire ultra low-*k* materials with much lower dielectric constant. By decreasing material density, the desirable dielectric constant could be achieved but the deterioration of mechanical properties was also accompanied, which made multi-level integration much more difficult. Since the thermo-mechanical properties of porous low-*k* films were highly dependent on the matrix materials, it was necessary to optimize the composition of the copolymers. Based on the investigation, the mechanical strength compared to dielectric constant seemed to be excellent when BTMSE content to MTMS was approximately 30%. More detailed investigations about this topic are under progress.

References

1. International Technology Roadmap for Semiconductors (2003) Semiconductor Industry Association, San Jose, CA
2. Padovani AM, Rhodes L, Allen SAB, Kohl PA (2002) J Electrochem Soc 149:F149
3. Padovani AM, Riester L, Rhodes L, Allen SAB, Kohl PA (2002) J Electrochem Soc 149:F171
4. Toivola Y, Kim S, Cook RF, Char K, Lee J-K, Yoon DY, Rhee H-W, Kim SY, Jin MY (2004) J Electrochem Soc 151:F45
5. Cook RF, Liniger EG (1999) J Electrochem Soc 146:4439
6. Toivola Y, Thurn J, Cook RF (2002) J Electrochem Soc 149:F9
7. Kim S, Toivola Y, Cook RF, Char K, Chu S-H, Lee J-K, Yoon DY, Rhee H-W (2004) J Electrochem Soc 151:F37
8. Oliver WC, Pharr GM (1992) J Mater Res 7:1564
9. Zhao J-H, Malik I, Ryan T, Ogawa ET, Ho PS, Shih W-Y, McKerrow AJ, Taylor KJ (1999) Appl Phys Lett 74:944
10. Shaffer EO, Mills ME, Hawn DD, Van Gestel M, Knorr A, Gundlach H, Kumar K, Kaloyeros AE, Geer RE (1998) Mater Res Soc Symp Proc 511:133
11. Ho PS, Leu J, Morgan M, Kiene M, Zhao J-H, Hu C (2003) In: Murarka SP, Eizenberg M, Shina AK (eds) Interlayer dielectrics for semiconductor technologies. Elsevier Academic Press, London, p 37
12. Flannery CM, Murray C, Streiter I, Shultz SE (2001) Thin Solid Films 388:1
13. Ma Q (1997) J Mater Res 12:840
14. Vella JB, Adhihetty IS, Junker K, Volinsky AA (2003) Int J fracture 119/120:487

15. Nagai H, Maekawa K, Iwashita M, Muramatsu M, Kubota K, Hinata K, Kokubo T (2004) In: Proceedings IITC, p 145
16. Oh W, Shin TJ, Ree M, Jin MY, Char K (2002) Macromol Chem Phys 203:801
17. Lee H-J, Lin EK, Wang H, Wu W-L, Chen W, Moyer ES (2002) Chem Mater 14:1845
18. Nay RJ, Warren OL, Yang D, Wyrobek TJ (2004) Microelectron Eng 75:103
19. Hay JC, Liniger EG, Liu X-H (2000) In: Mittal KL (ed) Adhesion measurements of films and coatings, 2nd edn. VSP, Utrecht, p 205